



Egyptian Knowledge Bank



***International Journal of Advances in Structural
and Geotechnical Engineering***

<https://asge.journals.ekb.eg/>

Print ISSN 2785-9509

Online ISSN 2812-5142

Special Issue for ICASGE'19

***Bearing Capacity for Rock with Multiple Cavities
Below Shallow Foundations***

M. H. M. Rabie, M. A. Atia and R. Khedr

ASGE Vol. 03 (01), pp. 1-17, 2019

Bearing Capacity for Rock with Multiple Cavities Below Shallow Foundations

M. H. M. Rabie¹, M. A. Atia² and R. Khedr³

¹ *Professor of Geotechnical Engineering and Foundation, Faculty of Engineering at Mataria, Helwan University, Egypt;*

E-mail: m.rabie@take21.com

² *Lecture of Geotechnical Engineering and Foundation, Faculty of Engineering at Mataria, Helwan University, Egypt;*

E-mail: dmahmoud_75@yahoo.com

³ *Doctor of Geotechnical Engineering and Foundation, Faculty of Engineering, Egyptian Russian University. (Projects Manager), in Housing Department at New Valley, Egypt;*

E-mail: raafatkhedr@yahoo.com

ABSTRACT

Failure mechanisms of shallow foundations resting on rock with isolated multiple cavities was studied under uniaxial compressive conditions. Various variables were investigated and those were: rock properties, cavity size, cavity depth, and cavity location. Upper bound mechanism had been derived depending on failure mechanisms obtained from experimental results in this study. One upper bound mechanism was made for circular shallow foundation resting on rock with spherical isolated multiple cavities and this was sidewall failure mechanism. The ultimate collapse pressure estimation equation for shallow foundation resting on rock containing multiple cavities was developed as a function of rock properties, and the geometry of the mechanism. This equation can be used to determine the ultimate bearing capacity of shallow foundation resting on rock with multiple cavities. The results were compared with previous works results. There was a good agreement between results.

Keywords: Bearing Capacity, Rock, Cavity, Shallow Foundations.

1. Introduction

Presence of cavities in a rock mass may affect on its mechanical behaviour, and failure mechanism. The correct estimation of the failure mechanisms of rock plays an important role in the design of foundations in it. The design of rock foundations includes, bearing capacity and settlement analyses. The bearing capacity equations represent either empirical or semi-empirical approximations of the ultimate bearing capacity and are dependent on the mode of potential failure. So that selection of an appropriate equation must anticipate likely modes of potential failure. (Egyptian Code for Foundation on Rock, 2008).

ICASGE'19

25-28 March 2019, Hurghada, Egypt

Sowers (1979), Kulhawy and Goodman (1980), suggested typical failure modes according to rock mass conditions. Failure modes were described according to four general rock mass conditions: intact, jointed, layered, and fractured. Wang and Hsieh (1987) developed three failure mechanisms that are considered to model the collapse of strip footing centered above a single circular void by using upper bound theorem of limit analysis, as shown in figure (1).

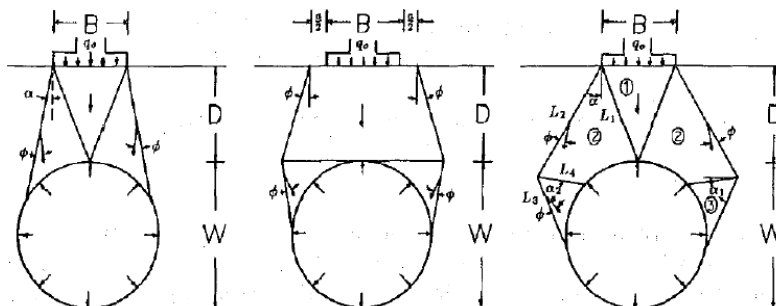


Fig. 1: Failure mechanisms (after Wang and Hsieh 1987)

Kiyosumi et al. (2011) reported the results of laboratory scale model tests of strip footing on stiff ground with continuous square voids and stated three upper-bound mechanisms for a single void from the experiments those were : roof failure, sidewall failure, and combined failure, as shown in figure (2). The upper-bound solutions of bearing capacity for strip footing were respectively derived.

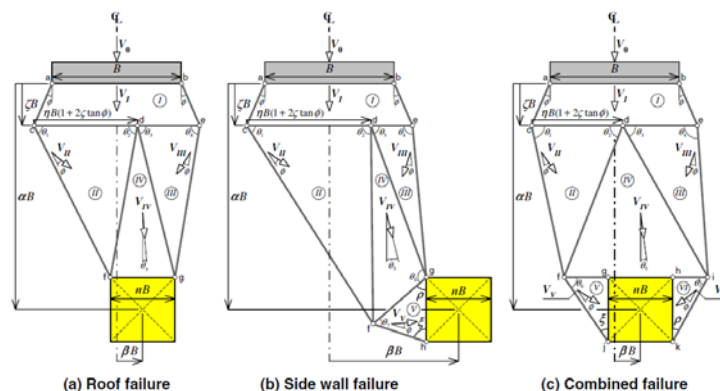


Fig. 2: Upper-bound mechanisms (after Kiyosumi et al. 2011)

The ultimate bearing capacity (q_{ub}) for the upper-bound solution is defined by the total rate of energy dissipation (D) and the total rate of work done (W) as

$$q_{ub} = (D - W) / V_o B$$

The total rate of energy dissipation (D) and the total rate of work done (W) for the sidewall failure mode are written by

$$D = cV_0(\cos \phi \{2l_{ac} + [l_{cf} / \sin(\theta_1 - \phi)] + [l_{eg} / \sin(\theta_4 - \phi)]\} \\ + l_{fh} \sin(\theta_1 + \theta_2 - \phi) \cos(\theta_6 - \theta_5 - \theta_3) / \sin(\theta_1 - \phi) \sin(\theta_7 - \phi) \cos(\theta_5 - \theta_2)\} + l_{cd} |1 / \tan(\theta_1 - \phi)| + l_{de} |1 / \tan(\theta_4 - \phi)| \\ + l_{df} / \sin(\theta_1 - \phi) | \sin(\theta_1 + \theta_2 - \phi) \tan(\theta_5 - \theta_2) - \cos(\theta_1 + \theta_2 - \phi) | + l_{dg} / \sin(\theta_4 - \phi) | \sin(\theta_3 + \theta_4 - \phi) \tan(-\theta_5 - \theta_3) \\ - \cos(\theta_3 + \theta_4 - \phi) | + l_{fg} \sin(\theta_1 + \theta_2 - \phi) / \sin(\theta_1 - \phi) \cos(\theta_5 - \theta_2) | - \sin(\theta_6 - \theta_5 - \theta_3) - \cos(\theta_6 - \theta_5 - \theta_3) / \tan(\theta_7 - \phi) |)$$

$$W = \gamma V_0 \{A_I + A_{II} + A_{III} + \sin(\theta_1 + \theta_2 - \phi) / \sin(\theta_1 - \phi) \cos(\theta_5 - \theta_2) \\ \times [A_{IV} \cos \theta_5 + A_V \cos(\theta_6 - \theta_5 - \theta_3) \cos(\xi + \phi) / \sin(\theta_7 - \phi)]\}$$

Where c and ϕ are strength parameters; γ is unit weight of the soil; B is footing width; $l_{ac} \sim l_{fg}$ are side lengths of the various zones; θ_{1-7} are angles of zones; θ_5 is inclination of V_{IV} ; and $A_I \sim A_V$ are areas of zones.

The expressions for the side lengths of the various zones are obtained from

$$l_{ac} = cB / \cos \phi, \quad l_{cd} = \eta B(2\zeta \tan \phi + 1), \quad l_{de} = B(1 - \eta)(2\zeta \tan \phi + 1) \\ l_{cf} = B \sqrt{\{\beta - n[(1/2) + \tan \xi \tan \rho / \tan \xi + \tan \rho] + \zeta \tan \phi + (1/2)\}^2 + \{\alpha + n[(1/2) - \tan \rho / (\tan \xi + \tan \rho)] - \zeta\}^2} \\ l_{df} = B \sqrt{\{\beta - n[(1/2) + \tan \xi \tan \rho / (\tan \xi + \tan \rho)] + \zeta \tan \phi(1 - 2\eta) - [\eta + (1/2)]\}^2 + \{\alpha + n[(1/2) - \tan \rho / (\tan \xi + \tan \rho)] - \zeta\}^2} \\ l_{dg} = B \sqrt{[\beta + \zeta \tan \phi(1 - 2\eta) - \eta - (1/2)(n - 1)]^2 + (\alpha + n/2 - \zeta)^2} \quad l_{eg} = B \sqrt{[\beta - \zeta \tan \phi - (1/2)(n + 1)]^2 + (\alpha + n/2 - \zeta)^2} \\ l_{fg} = nB \sqrt{[\tan \xi \tan \rho / (\tan \xi + \tan \rho)]^2 + [\tan \rho / (\tan \xi + \tan \rho) - 1]^2} \quad l_{fh} = nB \tan \rho / (nB \tan \rho / (\tan \xi + \tan \rho) \sqrt{\tan^2 \xi + 1})$$

The expressions for angles of zones

$$\theta_1 = \cos^{-1} \{B\{\beta - n[(1/2) + \tan \xi \tan \rho / (\tan \xi + \tan \rho)] + [\zeta \tan \phi + (1/2)] / l_{cf}\}\} > \phi \\ \theta_2 = \cos^{-1} \{B\{-\beta + n[(1/2) + \tan \xi \tan \rho / (\tan \xi + \tan \rho)] + \zeta \tan \phi(2\eta - 1) + [\eta - (1/2)] / l_{df}\}\} \\ \theta_3 = \cos^{-1} \{B[\beta + \zeta \tan \phi(1 - 2\eta) - \eta + (1/2)(1 - n)] / l_{dg}\} \\ \theta_4 = \cos^{-1} \{B[-\beta + \zeta \tan \phi + (1/2)(1 + n)] / l_{eg}\} > \phi \quad \theta_6 = 90 + \theta_3 - \rho \quad \theta_7 = (180 - \rho - \xi) > \phi$$

The expression for the areas of zones are calculated by

$$A_{II} = \sqrt{s_{II}(s_{II} - l_{cd})(s_{II} - l_{cf})(s_{II} - l_{df})}, \quad s_{II} = (l_{cd} + l_{cf} + l_{df}) / 2 \\ A_{III} = \sqrt{s_{III}(s_{III} - l_{de})(s_{III} - l_{eg})(s_{III} - l_{dg})}, \quad s_{III} = (l_{de} + l_{eg} + l_{dg}) / 2 \\ A_{IV} = \sqrt{s_{IV}(s_{IV} - l_{df})(s_{IV} - l_{dg})(s_{IV} - l_{fg})}, \quad s_{IV} = (l_{df} + l_{dg} + l_{fg}) / 2 \\ A_V = \sqrt{s_V(s_V - l_{fg})(s_V - l_{fh})(s_V - n \cdot B)}, \quad s_V = (l_{fg} + l_{fh} + n \cdot B) / 2$$

Most of previous studies of the bearing capacity of foundations above cavities have been investigated the behavior of cavities considering continuous shapes. Although it is recognized that the cavities exist in nature in continuous and isolated shape. Previous studies only considered the behaviour of single and double cavities of various shapes. Although it is recognized that the cavities exist in nature as single, double, and multiple cavities. The bearing capacity equation presented by previous studies were complex, very long and very difficult for application. This paper presents results of a series of laboratory model tests carried out on a circular shallow foundation resting on rock with isolated spherical multiple cavities, the

uniaxial compressive strengths of the tested rock were 6.7 Mpa and 20.12 Mpa. Simple upper-bound calculations were also presented to interpret the changes of bearing capacity observed because of the presence of the multiple cavities.

2. Laboratory model tests

2.1 Rock Like Materials

Natural materials such as, gypsum, and limestone powder were used to make Rock Like Materials containing cavities. In order to vary the compressive strength and density of rock, two mixtures were selected. The first selected mixtures named as group C, and the second mixture named as group L. The properties and classification of the two selected materials (group C and group L) are summarized in Table (1).

Table 1: Properties and classification of selected Rock Like Materials

Group	γ (KN/m ³)	q_u (MPa)	σ_t (MPa)	E (GPa)	ν	Classification
C	16	6.7	1.27	0.51	0.19	Very Low Density, Low Strength Like to Sedimentary Rocks
L	19.8	20.12	2.16	0.99	0.25	Low Density, Moderate Strength Like to Sedimentary Rocks

Model tests of cubic blocks are prepared in laboratory from rock like materials to simulate rock mass containing isolated, empty, spherical cavities. The dimensions of each block are 150 × 150 × 150 mm. The isolated empty spherical cavities is made from plastic. The model of shallow foundation resting on the block is a circular footing with 20 mm diameter and 10 mm thickness.

2.2 Testing Program

Testing program include two main groups C and L, which simulate two type of rock. Each group consists of two main test conditions as shown in figure (3) and tables (2) and (3) . The main test conditions are as follow :-

- (1) Circular shallow foundation resting on rock without cavities.
- (2) Circular shallow foundation resting on rock with multiple isolated cavities at distance with and offset from the axis of foundation.

ICASGE'19

25-28 March 2019, Hurghada, Egypt

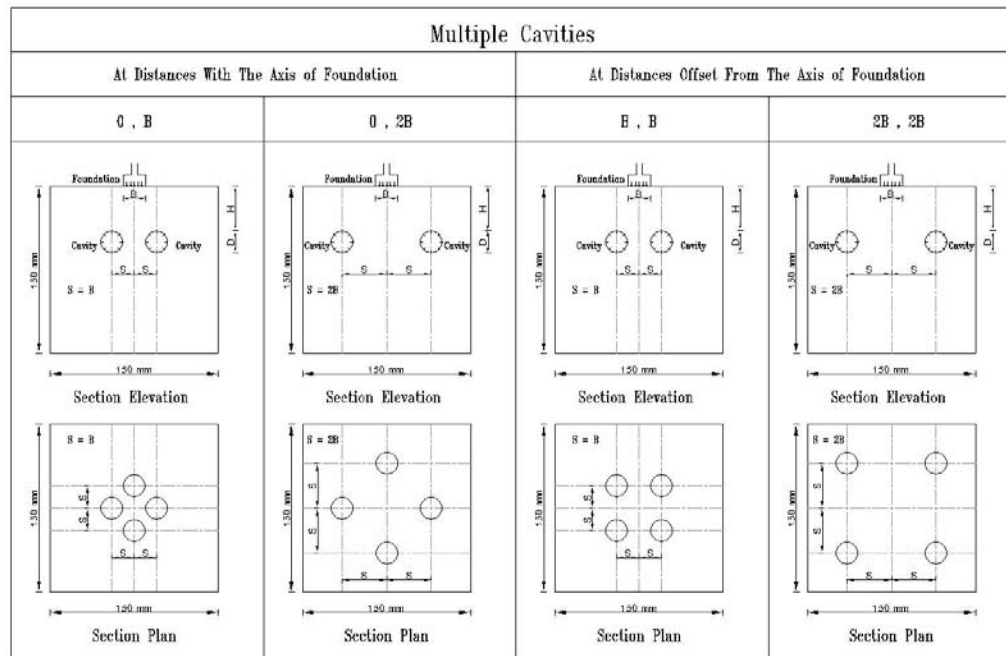


Fig. 3: Main test conditions

2.3 Preparation of the model test

222 cubic blocks are prepared in laboratory for 74 model tests of the two groups C and L. Model tests were characterized as homogenous and isotropic, also arrangement of cavities inside the blocks are symmetric. Model test preparation procedure are as follow :-

- (1) Two selected mixed materials were mixed and cast manually in steel mould with dimensions of $150 \times 150 \times 150$ mm.
- (2) Empty cavities with different sizes and depths were placed inside mixed materials in the mould by using steel stamps for detecting location and depth of cavities accurately.
- (3) All blocks were stored at laboratory chamber for 28 days after casting.

Table 2: Testing Program for group C

Number of cubic blocks	Cavity diameter D/B	Cavity depth H/B	Multiple Cavities			
			With the axis of foundation		Offset from the axis of foundation	
			$S = 0, B$	$S = 0, 2B$	$S = B, B$	$S = 2B, 2B$

ICASGE'19

25-28 March 2019, Hurghada, Egypt

4×3=12	0.5	1	C-1	C-2	C-3	C-4
4×3=12		2	C-5	C-6	C-7	C-8
4×3=12		4	C-9	C-10	C-11	C-12
4×3=12	0.75	1	C-13	C-14	C-15	C-16
4×3=12		2	C-17	C-18	C-19	C-20
4×3=12		4	C-21	C-22	C-23	C-24
4×3=12	1	1	C-25	C-26	C-27	C-28
4×3=12		2	C-29	C-30	C-31	C-32
4×3=12		4	C-33	C-34	C-35	C-36
3	C-W	Without Cavities				
111	Total number of blocks in 37 model test					

Table 3: Testing Program for group L

Number of cubic blocks	Cavity diameter D/B	Cavity depth H/B	Multiple Cavities			
			With the axis of foundation		Offset from the axis of foundation	
			S = 0,B	S = 0,2B	S = B,B	S = 2B,2B
4×3=12	0.5	1	L-1	L-2	L-3	L-4
4×3=12		2	L-5	L-6	L-7	L-8
4×3=12		4	L-9	L-10	L-11	L-12
4×3=12	0.75	1	L-13	L-14	L-15	L-16
4×3=12		2	L-17	L-18	L-19	L-20
4×3=12		4	L-21	L-22	L-23	L-24
4×3=12	1	1	L-25	L-26	L-27	L-28
4×3=12		2	L-29	L-30	L-31	L-32
4×3=12		4	L-33	L-34	L-35	L-36
3	L-W	Without Cavities				
111	Total number of blocks in 37 model test					

2.4 Test procedure

Test procedure were as follow :-

- (1) All blocks were weighted before testing.
- (2) Position of the foundation was detected at the block centerline before testing the models.
- (3) All models were tested in uniaxial compression, by using manual hydraulic jack. The blocks are loaded using a fixed lower platen and model of circular shallow foundation fixed with upper platen. Circular shallow foundation was situated at the center of block, the applied load was increased such that failure occurs; the load was recorded for each 0.25 mm settlement and the failure load "P" is recorded.

3. Results and Discussion

ICASGE'19

25-28 March 2019, Hurghada, Egypt

3.1 Shallow foundation resting on rock without cavities

The bearing pressure q_b for group C-w is 117.05 Mpa. Also the bearing pressure q_b for group L-w is 195.72 Mpa. Failure mechanism was shown in figures (4). It can be clearly seen that an irregular longitudinal splitting fracture for the tested blocks, this was due to unconfined compression for brittle rock. This is confirmed with Jaeger and Cook, 1979. From figures (4-a), and (4-c), it was noticed that the bearing capacity failure mechanism was a local shear failure initiated at the edge of the foundation as localized crushing and develops into active wedge below the foundation as a conical rigid block and slip surfaces. The slip surfaces do not reach the block surface. Localized shear failures were generally associated with brittle rock. This is a good agreement with results that obtained by Sowers (1979), Kulhawy and Goodman (1980).

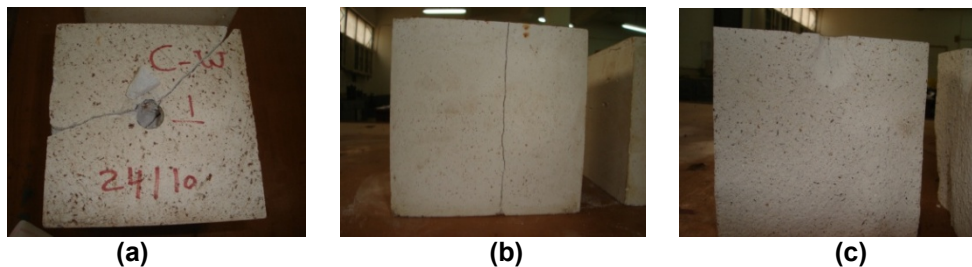


Fig. 4: Failure mechanism for rock without cavities of group C-w,
(a) conical active wedge (b) splitting fracture, (c) local shear failure

3.2 Shallow foundation resting on rock with multiple cavities

Four spherical cavities are positioned symmetrically in different locations from foundation center, as shown formally in figure (3). Size of cavities is considering by $D/B = 0.5, 0.75, 1$ and cavities depths are considering by $H/B = 1, 2, 4$. Radial distance from foundation center to cavity center is L . Where ($L/B = 1, 1.41, 2,$ and 2.82) for distances S equal to $(0, B), (B, B), (0, 2B),$ and $(2B, 2B)$ respectively. To clarify effect of multiple cavities location on foundation stability, it is presented as a relations between the ratio of (q_b/q_{bw}) and L/B for model tests of groups C and L, as shown in figures from (5) to (10). It could be noticed that the effect of multiple cavities location on bearing pressure is high in the large shallow cavities near the foundation center, (at $L/B = 1, 1.41$) and low in the cavities far from foundation center (at $L/B = 2, 2.82$). According to results, failure mechanisms for shallow foundation resting on rock containing a multiple cavities may be classified into four categories as follow :

3.2.1 Small shallow multiple cavities near the foundation center :

This category include multiple cavities with size of ($D/B = 0.5$), at depths of ($H/B = 1, 2$), in locations of [$S = (0, B), (B, B)$], and at radial distances from foundation center of ($L/B = 1, 1.41$), for groups of (C-1, C-3, C-5, C-7, L-1, L-3, L-5, and L-7).

ICASGE'19

25-28 March 2019, Hurghada, Egypt

It is noticed that the reduction in bearing pressure is low which range between 17.05 %, and 11.48 % for model tests of group C. While the reduction in bearing pressure range between 7.84 %, and 5.88 % for model tests of group L. The reason of low reduction in bearing pressure is arching effect of small size cavities. Small cavities may be bridge the lateral pressure from foundation on cavity sidewall to the surround rock mass. Also, because of the cavities are located near the foundation center, and the thickness of rock mass cover below foundation is thin, this lead to the rock mass in critical region is small, which can hold low resistance. So with continue pressure, gradually sidewall collapse is happened. Failure mechanism for this group is a splitting failure, with sidewall failure of cavities, as shown in figure (11). Local shear failure initiated at the edge of the foundation as localized crushing and develops into rigid block as a conical wedge below the foundation. Conical wedge is moving vertically downward and dissipating the bonds between vertical faces of the conical block and the surrounding rock mass, which compress on the cavities walls then break it causing sidewall failure of cavities, after that the block is fail.

3.2.2 Large shallow multiple cavities near the foundation center :

This category contain multiple cavities with sizes of ($D/B = 0.75, 1$), at depths of ($H/B = 1, 2$), in locations of [$(S = (0, B), (B, B))$], and at radial distances from foundation center of ($L/B = 1, 1.41$), for groups of (C-13, C-15, C-17, C-19, C-25, C-27, C-29, C-31, L-13, L-15, L-17, L-19, L-25, L-27, L-29, and L-31). It is observed that the reduction in bearing pressure is high which range between 70.49 %, and 19.67 % for model tests of group C. While the reduction in bearing pressure for model tests of group L range between 34 %, and 3.23 %. The high reduction in bearing pressure is due to presence of Large cavities in critical region below foundation. Large cavity couldn't bridge the lateral pressure to surround rock mass, so the sidewall collapse is happened, especially when the cavities are situated near the foundation center, and at thin rock mass cover.

ICASGE'19

25-28 March 2019, Hurghada, Egypt

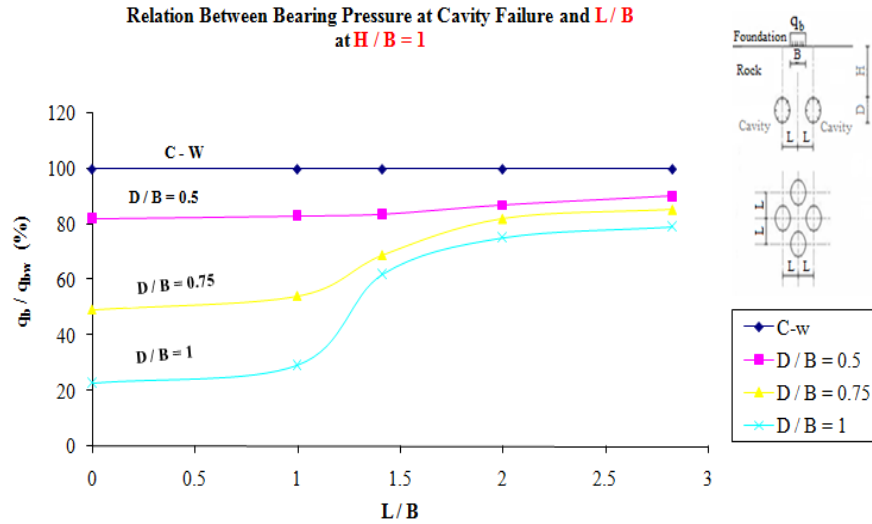


Fig. 5: Relation between bearing pressure at cavity failure and L/B for multiple cavities, at $H/B = 1$ for group C

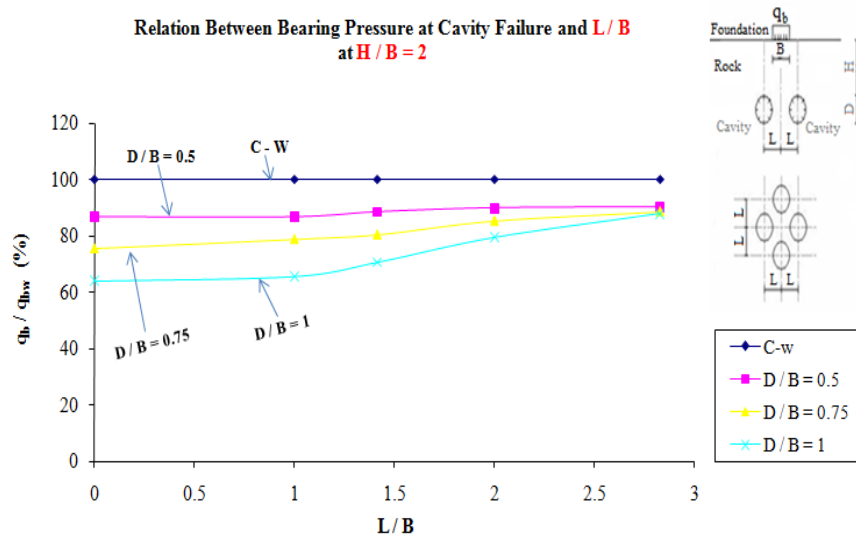


Fig. 6: Relation between bearing pressure at cavity failure and L/B for multiple cavities, at $H/B = 2$ for group C

ICASGE'19

25-28 March 2019, Hurghada, Egypt

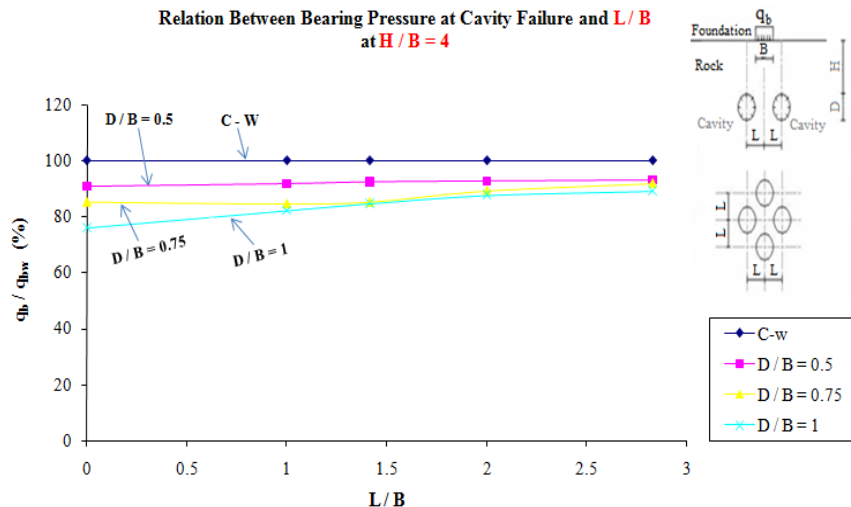


Fig. 7: Relation between bearing pressure at cavity failure and L/B for multiple cavities, at $H/B = 4$ for group C

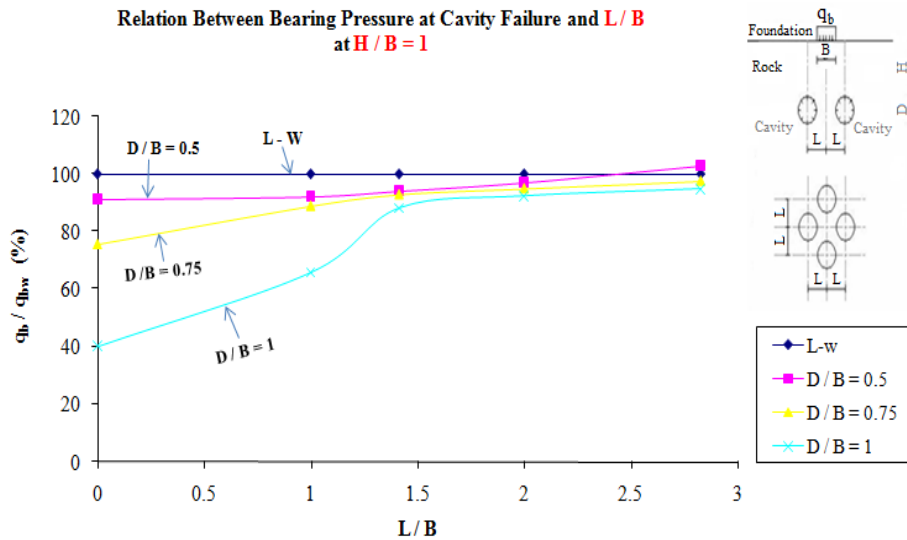


Fig. 8: Relation between bearing pressure at cavity failure and L/B for multiple cavities, at $H/B = 1$ for group L

ICASGE'19

25-28 March 2019, Hurghada, Egypt

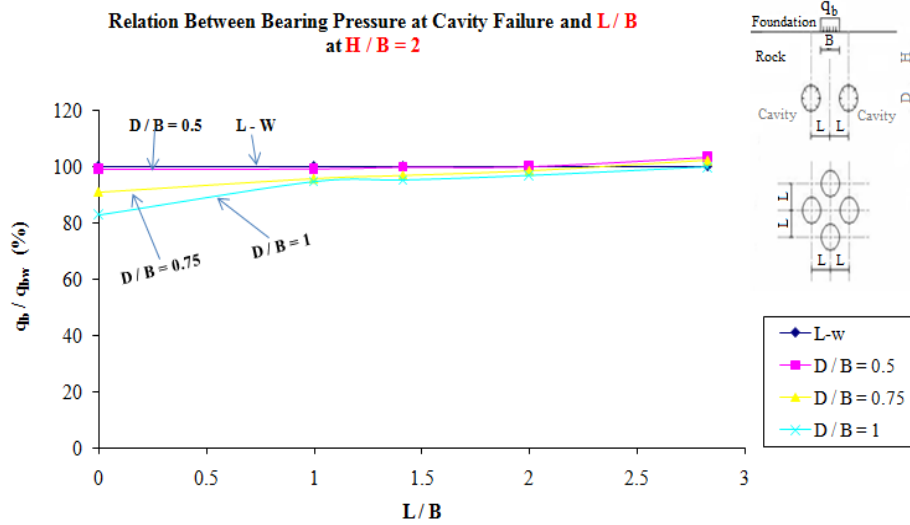


Fig. 9: Relation between bearing pressure at cavity failure and L/B for multiple cavities, at $H/B = 2$ for group L

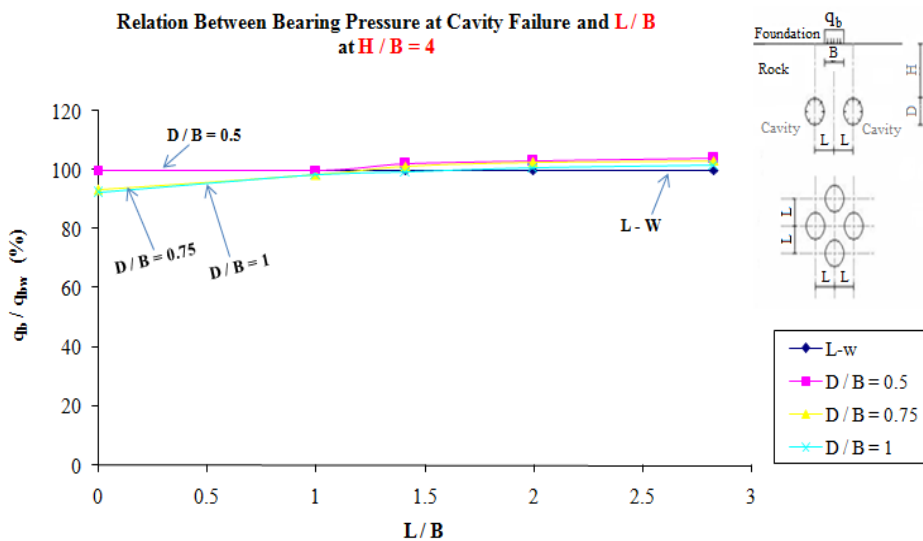


Fig. 10: Relation between bearing pressure at cavity failure and L/B for multiple cavities, at $H/B = 4$ for group L

ICASGE'19

25-28 March 2019, Hurghada, Egypt

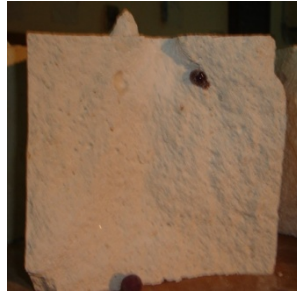


Fig. 11: Failure mechanism for multiple cavities of group L-1

Failure mechanism is a splitting failure, with sidewall failure of cavities, as illustrated in figure (12). Local shear failure initiated at the edge of the foundation as localized crushing and develops into a conical wedge below the foundation. Conical wedge is moving vertically downward and dissipating the bonds between vertical faces of the conical block and the surrounding rock mass. Another cylindrical rigid block is formed between conical wedge and cavity wall as shown in figure (12-b). Cylindrical rigid block compress on the cavity wall then break it producing sidewall failure of cavities, after that the block is fail.



(a) C-13



(b) C-15

Fig. 12: Failure mechanism for multiple cavities (a) C-13, (b) C-15

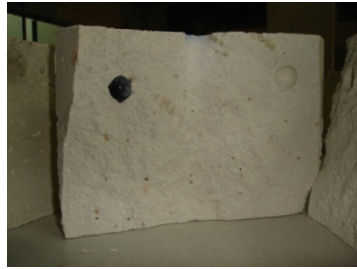
3.2.3 Shallow multiple cavities far from foundation center :

This category consist of multiple cavities with sizes of ($D/B = 0.5, 0.75, 1$), at depths of ($H/B = 1, 2$), in locations of [$S = (0, 2B), (2B, 2B)$], and at radial distances from foundation center of ($L/B = 2, 2.82$), for groups of (C-2, C-4, C-6, C-8, C-14, C-16, C-18, C-20, C-26, C-28, C-30, C-32, L-2, L-4, L-6, L-8, L-14, L-16, L-18, L-20, L-26, L-28, L-30, and L-32). The reduction in bearing pressure is starting to disappear gradually, which range between 24.59 %, and 9.84 % for model tests of group C. While the reduction in bearing pressure for model tests of group L range between 7.41 %, and 0 %. The gradually disappearing of reduction in bearing pressure is due to the cavities are positioned away gradually from the critical region, although the cavities are at thin rock mass cover. The radial

ICASGE'19

25-28 March 2019, Hurghada, Egypt

distance between foundation center and cavities centers is wide, so that rock mass can hold high resistance. Failure mechanism is a splitting failure, without cavities failure, as illustrated in figure (13). Local shear failure initiated at the edge of the foundation and develops into conical wedge, below the foundation, moving vertically downward and dissipating the bonds between vertical faces of the conical block and the surrounding rock mass without cavities failure.



(a) L-20



(b) C-30

Fig. 13: Failure mechanism for multiple cavities (a) L-20, (b) C-30

3.2.4 Deep multiple cavities :

This category involve multiple cavities with sizes of ($D/B = 0.5, 0.75, 1$), at depths of ($H/B = 4$), in locations of [$S = (0, B), (0, 2B), (B, B), (2B, 2B)$], and at radial distances from foundation center of ($L/B = 1, 1.41, 2, 2.82$), for groups of (C-9, C-10, C-11, C-12, C-21, C-22, C-23, C-24, C-33, C-34, C-35, C-36, L-9, L-10, L-11, L-12, L-21, L-22, L-23, L-24, L-33, L-34, L-35, and L-36). The reduction in bearing pressure is very low, which range between 17.82 %, and 6.88 % for model tests of group C. While the reduction in bearing pressure for model tests of group L range between 1.79 %, and 0 %. The cavities are outside the critical region. This is because they are sited far away from the foundation bottom, the rock mass thickness below the foundation can hold more shear strain before failure, beside the arching marked shearing resistance of rock.

Failure mechanism is a splitting failure, without cavities failure, as illustrated in figure (14). Local shear failure initiated at the edge of the foundation as localized crushing and develops into conical wedge, below the foundation, moving vertically downward and dissipating the bonds between vertical faces of the conical block and the surrounding rock mass without cavities failure.



(a) C-23



(b) C-33



(c) C-34

Fig. 14: Failure mechanism for multiple cavities (a) C-23, (b) C-33, (c) C-34

4. Upper Bound Mechanism Analysis

Based on the failure mechanisms, that obtained from experimental results in this study. one upper bound mechanism made for circular shallow foundation resting on rock containing spherical isolated multiple cavities is cavity sidewall failure mechanism.

For this failure mechanism, the rate of energy dissipation along active wedge movement, the rate of work done by foundation pressure, and rock weight are obtained. By equating the rate of energy dissipated and rate of work done, the equation for foundation collapse pressure as a function of foundation width, cavity size, cavity depth, cavity location, and rock properties is formulated. Each equation contained one or more variables that define the geometry of failure mechanism. Not that, in the equations, the pressure inside the cavity is assumed to be zero. Also the external work done by the rock weight is expressed in terms of volume of rock mass involved, since the three-dimensional analysis is made. Simple mathematical models are used for study the global equilibrium for summation of vertical forces (external and inner forces). The collapse load is equal to the difference between plastic power and force power ($D_i - D_e$).

4.1 Cavity Sidewall Failure Mechanism

This mechanism include shallow multiple cavities near the foundation center with sizes of ($D/B = 0.5, 0.75, 1$), at depths of ($H/B = 1, 2$), in locations of [$(S = (0, B), (B, B))$], and at radial distances from foundation center of ($L/B = 1, 1.41$), for groups of (C-1, C-3, C-5, C-7, C-13, C-15, C-17, C-19, C-25, C-27, C-29, C-31, L-1, L-3, L-5, L-7, L-13, L-15, L-17, L-19, L-25, L-27, L-29, and L-31), as shown in figures (11), and (12).

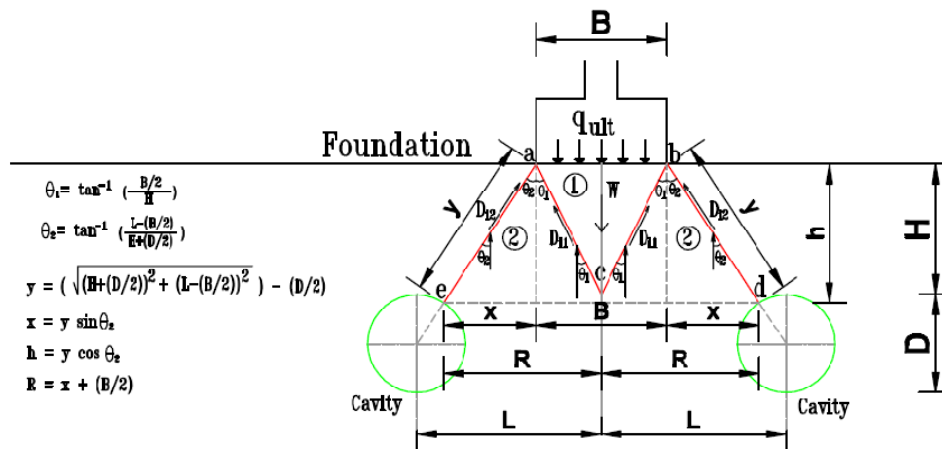


Fig. 15: Upper-bound mechanism for cavity sidewall failure mechanism of shallow multiple cavities near to foundation centre, at $(D/B = 0.5, 0.75, 1, H/B = 1, 2, L/B = 1, 1.41)$

Figure (15) show the upper-bound mechanism for cavity sidewall failure mechanism of shallow multiple cavities near the foundation centre.

$$q_{ult} = (1/A) \{ [q_u \{ \cos \theta_1 [\pi (B/2) ((B/2)^2 + H^2)^{0.5}] + \cos \theta_2 [\pi y (R + (B/2))] \}] - [\gamma \{ (\pi/3) (h) [R^2 + (B/2)^2 + R (B/2)] \}] \}$$

Where :

q_{ult} = Ultimate bearing capacity.

A = Foundation area.

q_u = Uniaxial compressive strength of intact rock core.

B = Foundation width.

H = Cavity depth below foundation.

γ = Density of the rock material

D = Cavity diameter.

L = Radial distance from foundation center to cavities centers.

5. Verification of results

It is important to check the results against those from other previous works where possible. Figure (16) present a comparison between present study results, and results of Kiyosumie et al., 20011 for small shallow multiple cavities ($D/B = 0.5, H/B = 0.5$). It is noticed that the curves are similar, and approach together. The results of Kiyosumie et al., 2011 are verified the results of present study.

ICASGE'19

25-28 March 2019, Hurghada, Egypt

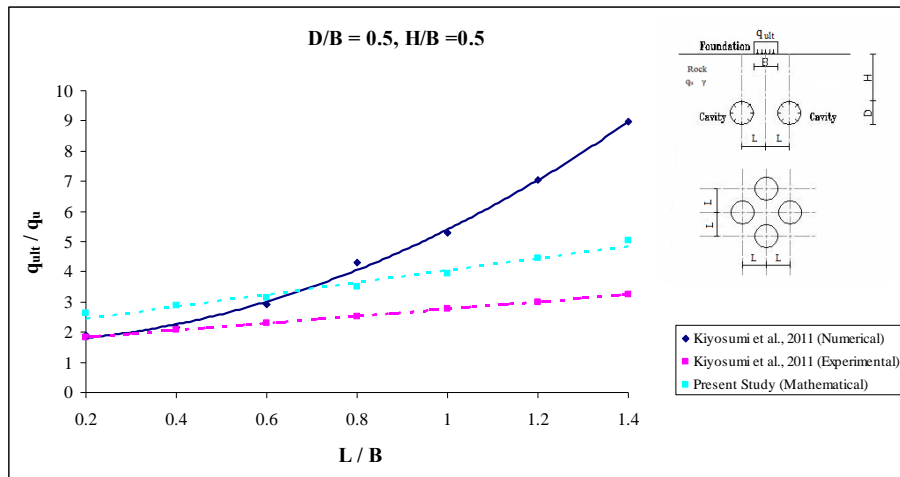


Fig. 16: Comparison between present study results, and results of Kiyosumi et al., 2011

6. Conclusions

- 1- Failure mechanism for rock without cavity was longitudinal splitting fracture, this is due to uniaxial compression for brittle rock. This is confirm with Jaeger and Cook ,1979.
- 2- Bearing capacity failure mechanism for rock without cavity was a local shear failure. Localized shear failures are generally associated with brittle rock. This is a good agreement with results that obtained by Sowers (1979) and Kulhawy and Goodman (1980).
- 3- Failure mechanisms for rock containing multiple cavities was a splitting Failure, this was due to uniaxial compression for brittle rock.
- 4- The upper bound failure mechanism for shallow foundation resting on rock containing multiple cavities is cavity sidewall failure for shallow multiple cavities near the foundation center.
- 5- The ultimate collapse pressure estimation equation for shallow foundation resting on rock containing multiple cavities was developed as a function of rock properties, and the geometry of the mechanism. This equation can be used to determine the ultimate bearing capacity of shallow foundation resting on rock with cavities.

7. REFERENCES

- (1) "Egyptian Code for Soil Mechanics and Foundation, Ten part, Foundation on Rock", (2008), Housing and Building National Research Center Cairo, Egypt.
- (2) Jaeger J. C, Cook N. G. W. "Fundamentals of rock mechanics" [M]. 3rd edition. London: Chapman and Hall, (1979).
- (3) Kiyosumi M, Kusakabe O, Ohuchi M. ,(2011). "Model tests and analyses of bearing capacity of strip footing on stiff ground with voids". Journal of Geotechnical and Geoenvironmental Engineering;137, pp. 363 –375.
- (4) Kulhawy, F. H. and Goodman, R. E., (1980), "Design of foundations on discontinuous rock", Proc. Int. Conf. Structural Foundations on Rock, Sydney, 1, p.p. 209-220.
- (5) Sowers, G. F., (1979), "Introductory Soil Mechanics and Foundations: Geotechnical Engineering" (4th edn), MacMillan, New York.
- (6) Sowers, G. F. (1996), "Building on sinkholes, design and construction of foundations in karst terrain". ASCE Press, Reston (out of print).
- (7) Terzaghi, K., "Arching in Ideal Soils," Chapter 5, Theoretical Soil Mechanics, John Wiley and Sons, Inc., New York, N. Y., (1943), pp. 66-76.
- (8) Wang M. C., Hsieh C. W., (1987). "Collapse load of strip footing above circular void". J Geotech Eng;113, pp. 511– 515.

قدرة التحمل لصخر ذي تكهفات متعددة أسفل الأساسات السطحية

الملخص بالعربي

تم إجراء دراسة معملية لاستكشاف تأثير التكهفات المنعزلة بالتربة الحجرية علي السلوك الميكانيكي و أنماط الانهيار للصخر ذي التكهفات أسفل الأساسات السطحية. و قد تم إجراء التحميل بالضغط المحوري علي نماذج الاختبار في هذه الدراسة. كما تم دراسة تأثير العديد من المتغيرات و هي : خواص الحجر و حجم التكهفات و عمقها و موقعها من مركز القاعدة. و تم إجراء الدراسة علي مجموعة مكونة من أربعة تكهفات موزعة بالتماثل حول مركز القاعدة. و بالاعتماد علي نتائج الدراسة المعملية تم استنتاج نمط واحد للانهيار و هو عبارة عن انهيار لجوانب التكهفات السطحية أسفل القاعدة الموجودة بالقرب من مركز القاعدة. كما تم استنتاج معادلة حساب قدرة التحمل القصوى للصخر ذي التكهفات المتعددة حسب نمط الانهيار المذكور عاليه. و للتأكد من دقة نتائج المعادلة المستنتجة تم مقارنتها بنتائج أحد الباحثين السابقين و تلاحظ التوافق بين جميع النتائج.